Process strategies for laser cutting of electrodes in lithium-ion battery production

Cite as: J. Laser Appl. **33**, 012006 (2021); https://doi.org/10.2351/7.0000335
Submitted: 30 November 2020 . Accepted: 30 November 2020 . Published Online: 18 December 2020

Johannes Kriegler, Moritz Binzer, and Michael F. Zaeh

Journal of Laser Applications ARTICLE scitation.org/journal/jla

Process strategies for laser cutting of electrodes in lithium-ion battery production

Cite as: J. Laser Appl. 33, 012006 (2021); doi: 10.2351/7.0000335
Submitted: 30 November 2020 · Accepted: 30 November 2020 ·
Published Online: 18 December 2020

Johannes Kriegler,[a] Moritz Binzer, and Michael F. Zaeh

AFFILIATIONS

Institute for Machine Tools and Industrial Management, Technical University of Munich (TUM), Boltzmannstraße 15, 85748 Garching, Germany

Note: Paper published as part of the special topic on Proceedings of the International Congress of Applications of Lasers & Electro-Optics 2020.

[a]**Author to whom correspondence should be addressed; electronic mail:** johannes.kriegler@iwb.tum.de

ABSTRACT

The growing competition in electric mobility is leading to an increased demand for inexpensive, high-performance lithium-ion batteries. In order to meet both objectives, optimization of the entire production chain is indispensable. In this work, the laser cutting of electrodes as one of the core processes in large-format battery production is addressed. A comprehensive literature review on the boundary conditions and the relevant quality characteristics of the separation process is presented. Furthermore, experimental findings regarding the dependency between cutting edge quality and achievable process speed of pulsed and continuous wave fiber lasers in the near infrared spectrum are compared. Finally, the design of customized cutting strategies based on multiple laser scan cycles is shown and the potential for the implementation in the battery production is discussed.

Key words: Laser cutting, Electrodes, Lithium-ion batteries, Graphite, Copper, Foils, Process strategies, Battery production

I. INTRODUCTION

Due to environmental, economic, and sociopolitical reasons, the automotive sector is subject to fundamental changes by means of electrification. Lithium-ion batteries (LIBs) are currently the main energy storage technology for electric vehicles and are key to fulfilling the standards postulated by the automotive market.[1] Since the cells represent approximately 65% of the cost of a battery-pack,[2] LIB production is one of the major fields of interest for car manufacturers worldwide. Over the past 30 years, extensive know-how in the production of small-scale LIBs for consumer electronics has been established, which is now being transferred to large-format cells.[3] In recent years, annual growth rates of around 25% have been recorded in the production of LIBs with an even higher expansion of the production volumes estimated for the upcoming years.[4] Several LIB manufacturers are currently planning factories with an output of more than 1 GWh storage capacity per year in Europe. By 2025, a worldwide annual production of more than 1 TWh storage capacity is predicted, which requires high-capacity production equipment.[4] To this day, the cost-efficient production of high-quality large-format cells at increasing throughput remains a challenge.[5] The complexity of the process chain results in significant scrap rates.[6] For future competitiveness, the entire battery value chain must be optimized.[7] While the continuous processes in electrode manufacturing can be scaled up effectively, electrode cutting is more critical due to the sharp increase in individual components.[8] Consequently, a shortening of the cycle times is of great interest but must not lead to a reduction in electrode quality. For the contour cutting of electrodes, fine blanking and laser cutting are currently employed. The selection of the cutting method is determined by the required cutting quality, the process speed as well as the equipment and processing costs. This paper demonstrates how the selection of customized cutting strategies can create advantages for the laser process by improving both quality and speed.

II. BOUNDARY CONDITIONS FOR ELECTRODE CUTTING

A. Material characteristics

LIB electrodes are multilayer systems with porous active material layers coated double-sided on metallic current collectors. The

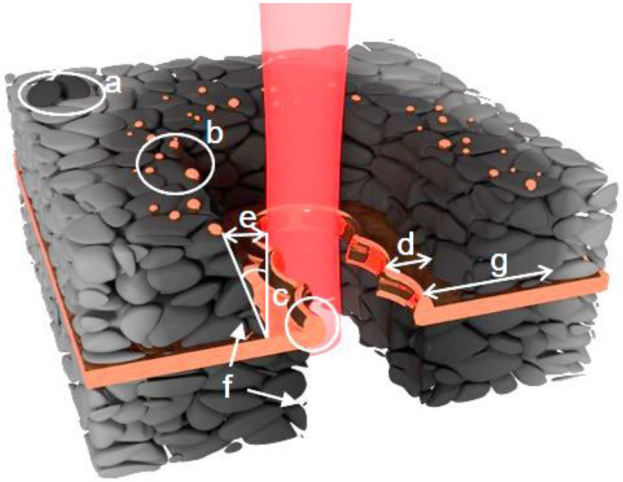

FIG. 1. Schematic representation of quality criteria with regard to laser cutting of electrodes; particles (a), spatters (b), burrs (c), clearance width w_c (d), chamfer width (e), unequal ablation of upper and lower layer (f), and heat affected zone (HAZ) (g).

coatings are multimaterial systems (see Fig. 1) consisting of active material particles that can accommodate lithium ions (>90 wt. %), binding agents (<5 wt. %), and conductive additives (<5 wt. %). On the anode side, a copper current collector (thickness: 6–10 μm[5] is usually combined with a graphite active material,[9] while on the cathode side, mainly lithium metal oxides are coated on aluminum foils (thickness: 12–20 μm).[5,10] Thicknesses of around 65–80 μm for the active material layers are employed for high energy cells.[11] However, higher material loadings are in development, as an increasing proportion of active material enhances the energy density on the cell level.[12] Typically, electrode porosities between 30 and 40% are used to enable high electric as well as ionic conductivity. The degree of electrode compaction is adjusted in a calendaring step after coating and drying of the electrode layers and must be considered when defining the laser parameters.[13] For emerging battery concepts with silicon-graphite anodes, laser cutting can be advantageous over blanking due to the abrasive behavior of the silicon particles.[14]

B. Productivity and economic viability

In a pouch cell factory with 1 GWh production capacity, more than 3×10^6 cutting operations are performed daily. On an industrial scale, fine blanking is widely used for contour cutting of cathodes and anodes.[15] The mechanical operating principle is accompanied by the wear of the punching tool, which leads to the reduced cut edge quality and downtime for tool replacement or repair. Since small cutting gaps of around 6 μm between the cutting punch and the die are needed for a high-quality mechanical separation process, considerable tooling and maintenance costs occur.[14] In addition, a new die must be fabricated if the cell format is changed, limiting the variability of the production line. These disadvantages open up opportunities for remote laser cutting as a noncontact alternative. The geometric flexibility within the range of the scan-field allows a quick modification of the electrode format. For these reasons, the mechanical process is increasingly replaced by laser cutting. In general, cutting speeds of 1 m/s are proposed for competitiveness with fine blanking,[16] which can reach up to ten strokes per second. If a large electrode format with dimensions of 150×300 mm^2 is requested, a circumference of 0.9 m originates (neglecting the electrode tab). As a consequence, similar process speeds to those of blanking would require a laser cutting speed of around 9 m/s. Depending on the operating hours, the break-even time of a laser cutting machine (higher investment costs) compared to a blanking system (higher operational costs) with equivalent output can vary, e.g., between 2 and 5 years for a laser system with a cutting velocity of 2.2 m/s.[17]

C. Quality criteria

In order to produce competitive LIBs with superior cost and performance, it is vital to minimize scrap rates by enhancing the quality of intermediate products. Due to the material costs and the large number of process steps, rejects have a major impact on the production costs. The further downstream a failure is in the process chain, the higher is the loss of value added by the preceding steps. Depending on the production scenario, around 60% of the total costs already have been incurred when cutting the electrodes to shape.[5] If a fault is not detected, even more added value of subsequent process steps are lost or early failure of the cell in operation is caused. Furthermore, defects from previous process steps can influence the cutting process. If the electrodes are corrugated after calendaring, an automated web edge control may not be able to find the coating edge, and precise cutting is prevented.[18] In Fig. 1, the relevant quality parameters for the laser cutting of battery electrodes are shown schematically.

Contaminations on the electrode surface must be avoided as delaminated active material particles [Fig. 1(a)] or spatters [Fig. 1(b)] can penetrate or scratch the sensitive insulator layers, leading to a mechanical failure of the separator and an internal short circuit.[19] Additionally, debris can block pores and deteriorate the ion transport.[20] By means of energy dispersive x-ray spectroscopy, the amount and extension of copper spatters around the cut edge can be classified.[21] For the inline detection of medium-sized particles ($\approx$30 μm) on the electrode surface, nondestructive inspection techniques, e.g., photo-optical detection, infrared detection, or active thermography can be integrated into the electrode cutting module.[22,23] Analogously to particles, melt superelevations and burrs [Fig. 1(c)] at the cut edge can pierce through the separator and provoke a short circuit.[24] While primarily the mechanical cutting process can lead to the formation of burrs, melt formation is caused by the photothermal impact of the laser process on the collector foils.[14] The different ablation thresholds of the current collector (e.g., copper) and the electrode coating (e.g., graphite) combined with the Gaussian intensity profile of the laser beam create a characteristic cutting geometry.[21] The resulting steplike cutting edge can be described via the clearance width w_c [Fig. 1(d)] and the chamfer width [Fig. 1(e)]. The ablated active material reduces the electrode loading and, therefore, the cell capacity. This is of particular interest in the case of small-format cells. Irregularities at the cut edge, like tapers or unequal ablation of the

upper and lower layer [Fig. 1(f)], can cause nonuniform cell aging. Hence, a w_c of less than 50 μm is targeted.[15] The heat affected zone (HAZ) describes the thermally influenced area [Fig. 1(g)]. To assess the degree of degradation, optical microscopy and scanning electron microscopy (SEM) are used.[25] In fact, as the polymer binders already evaporate at temperatures below 200 °C, e.g., PVDF at 178 °C,[26] a larger HAZ than detectable with optical methods is likely to appear reducing the mechanical integrity of the electrode.

D. Laser cutting in battery production

In industrial cell production, nanosecond (ns) laser sources with average powers in the range of 100–300 W are commonly used for laser separation of electrodes due to the combination of low heat impact, competitive cutting speeds, and reasonable costs. In the literature, a wide variety of beam sources is suggested[27] for laser separation of the electrodes in terms of operating type [continuous wave (cw), short-pulsed, ultrashort-pulsed], average power (a few watts up to kilowatts), and wavelength (ultraviolet, green, and infrared radiation). Despite the low absorption of the copper substrates on the anode side,[28,16] the wavelengths employed are usually in the infrared spectrum. Both cw lasers[13,29,30] and pulsed lasers[28,14,31,32,17,33,34,21] can meet the high demands on quality and cutting speed. Operating at cutting speeds of up to 10 m/s,[25,13] cw lasers are suitable for high volume production. To improve compliance with the quality characteristics like the HAZ, process strategies with multiple scan cycles proved to be adequate.[25] Short- and ultrashort-pulsed processes feature a low thermal energy input[35] into the electrode material and, thus, high cutting quality at an acceptable throughput rate.[31] The investigated pulse lengths mainly range in the ns-regime, as laser systems in this pulse spectrum are available at a high average power and rather low investment costs. Nevertheless, the technical development of high-power fiber lasers in the ultrashort pulse range is predicted to enhance the industrial relevance of these laser systems.[36,37] Overall, the selection of a suitable cutting strategy is complicated by the large variety of possible process regimes and the limited comparability of the existing literature. The electrode layers considered vary in composition, thickness, and porosity. Furthermore, no uniform measuring methods for the quality criteria presented can be found, impeding a classification of the published data. To overcome this issue the suitability of different beam sources for a selected material system is evaluated experimentally in the following.

III. EXPERIMENTAL APPROACH

A. Material

To ensure the comparability of the results, all experiments were conducted with the commercially purchased anode material. The electrode consisted of 95.8 wt. % natural graphite mixed with 1.0 wt. % of conductive carbon and 3.2 wt. % of binder. The active material was coated double-sided on a 10 μm copper foil, resulting in a total electrode thickness of 122 ± 2 μm. The porosity of the coating amounted to 40%. Further details on the material and the respective production processes were not disclosed by the supplier for reasons of confidentiality.

B. Laser systems

Three laser systems, as specified in Table I, were used for laser cutting of the graphite anodes. For all laser systems, beam guidance was realized through different galvanometer scanners. All test setups were equipped with a clamping device for a planar fixation, a cutting gap, and a suction system for the removal of ablated particles. No protective atmosphere was applied. However, the Nd:YAG fiber laser was located in a dry room, which did not affect the conducted experiments.

C. Analytics

For the evaluation of the cutting zone, a scanning electron microscope (SEM) (IT-200, JEOL, Germany) was used. The cutting width, the cutting depth, and the clearance width were measured with a laser scanning microscope (VK 9710, Keyence, Germany). To account for uneven edge shapes, each data point is based on averaged values from 50 parallel lines covering a total distance of 35 μm transversal to the cutting kerf.

IV. RESULTS AND DISCUSSION

A. Single-pass strategy

In this section, the ns pulsed laser system and the cw laser system described above are compared in terms of the achievable cutting velocity and cut edge quality. For this purpose, the

TABLE I. Characteristics of the utilized laser systems.

Laser system	YLP-HP-0.2-30-500-100LT	YLR-3000 SM	YLPP-25-3-50-R
Producer		IPG Photonics Corporation, USA	
Type	Nd:YAG fiber laser	Single-mode Yb fiber laser	Yb fiber laser
Operation mode	Pulsed	cw	Pulsed
Wavelength, λ	1064 nm	1070 nm	1030 nm
Max. laser power, P	100 W	3000 W	50 W
Pulse repetition rate, f	<500 kHz	–	<2750 kHz
Pulse duration, τ	30 ns	–	2 ps
Beam quality, M^2	1.1	1.3	1.2
Spot diameter, d_f	≈50 μm	≈60 μm	≈18 μm
Scan-field	350 × 380 mm^2	300 × 300 mm^2	40 × 40 mm^2

clearance width w_c was used as a quality criterion. Due to the differences in the optical setup and the varying ablation effects for pulsed and cw laser cutting, a comparison of the laser systems with respect to the line energy was neglected. While the reachable cutting speed v for the cw laser system only depends on the chosen laser power P, the performance of the ns pulsed laser system is also correlated to the pulse repetition rate f. At a constant power level, a higher f leads to lower pulse energies reducing the impact of every single pulse. As the temporal and spatial distance between the pulses is then reduced at a constant scanning speed v_s, an increased heat accumulation and higher thermal damage can occur.

To determine the maximum cutting speed, the scanning speed v_S was gradually raised for multiple parameter sets until no full-cut could be realized by a single scan cycle. The resulting cutting speeds and respective clearance width are shown in Fig. 2. When using the pulsed laser system, the maximum cutting speed increases linearly with the frequencies, which can be attributed to the ensuing higher pulse overlap. Due to the comparatively low pulse energies and pulse repetition rates, even at $f = 500$ kHz, no increased heat accumulation was observed. Overall, for the considered power levels of $P = 50$ W, $P = 75$ W, and $P = 100$ W, an accelerated cutting is achieved at an increasing laser power. Note that w_c was assessed for the maximum attainable cutting speeds of every parameter set. As higher laser powers correlate with higher cutting speeds, the energy input per area was not necessarily increased when enhancing the power level. For that reason, the parameter set for the maximum cutting speed of $v = 0.8$ m/s ($P = 100$ W, $f = 500$ kHz) also reached the lowest clearance width of $w_c = 42\,\mu$m [see Fig. 2(a)].

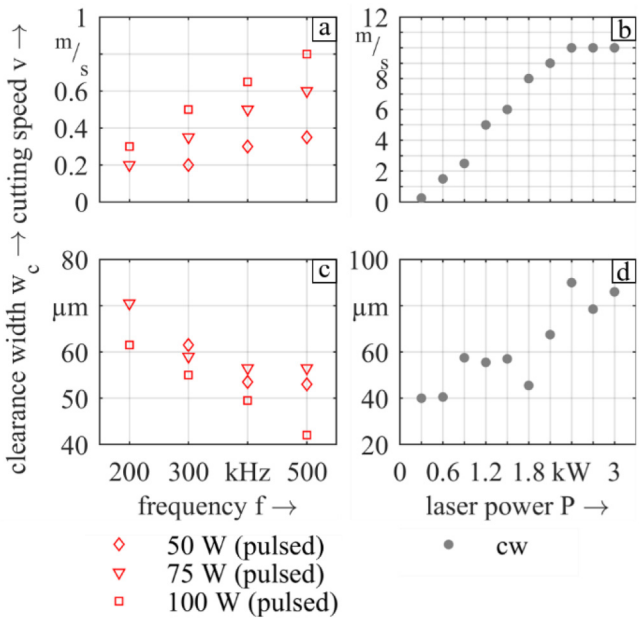

FIG. 2. Maximum cutting speed [(a) and (b)] and clearance width [(c) and (d)] for the pulsed laser system ($\tau = 30$ ns) [(a) and (c)] and the cw laser system [(b) and (d)].

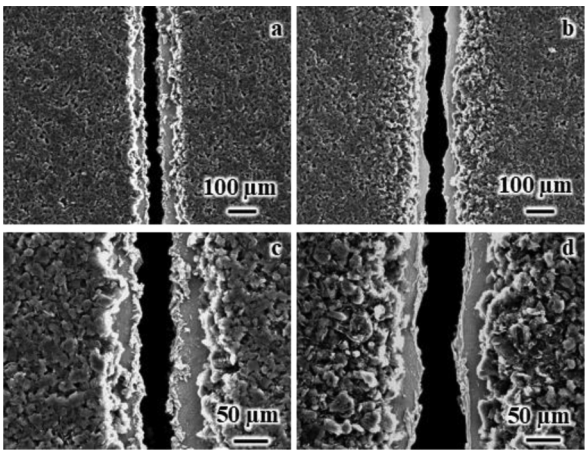

FIG. 3. SEM images of cutting kerfs in graphite anodes produced by the ns pulsed laser system ($P = 100$ W, $f = 500$ kHz, $v = 0.8$ m/s, $\tau = 30$ ns) [(a) and (c)] and the cw laser system ($P = 1800$ W, $v = 8.0$ m/s) [(b) and (d)].

As it can be seen in Fig. 2(b), cutting speeds of up to $v = 10$ m/s were achieved with the cw laser system. Faster processing could not be realized due to the limited line speed of the scanning system used. Hence, an increase in laser power beyond $P = 2.4$ kW did not lead to any further productivity. The smallest clearance width of $w_c = 40\,\mu$m was created at $P = 300$ W, while even at high cutting speeds, w_c remained comparatively small. At a laser power of $P = 1.8$ kW, a cutting speed of $v = 8$ m/s could be reached and still resulted in a low clearance width of $w_c = 45\,\mu$m representing a good trade-off between quality and productivity (see Fig. 3).

The fact that a minor clearance width could be achieved than at lower power levels can be attributed to the lower line energy, e.g., 225 J/m at $P = 1.8$ kW and $v_S = 8$ m/s in comparison to 267 J/m at $P = 1.6$ kW and $v_S = 6$ m/s, necessary to obtain a through cut. With the cw laser, a tenfold speed was achievable with only a slightly wider w_c. Overall, a more uniform cut edge can be observed for the ns pulsed process as displayed in Fig. 3 for selected parameter sets. This can be explained by a lower heat input and a less thermally dominated ablation mechanism.

B. Multipass strategy

The application of a multipass process strategy aims to reduce the thermal energy input, as the material is ablated layer by layer. By applying a higher scanning speed v_S, the line energy is reduced. The resulting lower material removal rates are counterbalanced by an increasing number of scan cycles. In this section, two cutting approaches are discussed. First, a multipass strategy with constant processing parameters is evaluated. Therefore, the number of scan cycles n was increased successively until a complete separation of the anode was achieved for different laser powers. With respect to the previous experiments, the pulsed laser system was evaluated for laser powers of $P = 100$ W at a pulse repetition rate of $f = 500$ kHz and the cw laser system for laser powers of $P = 300$ W, $P = 750$ W, and $P = 1200$ W.

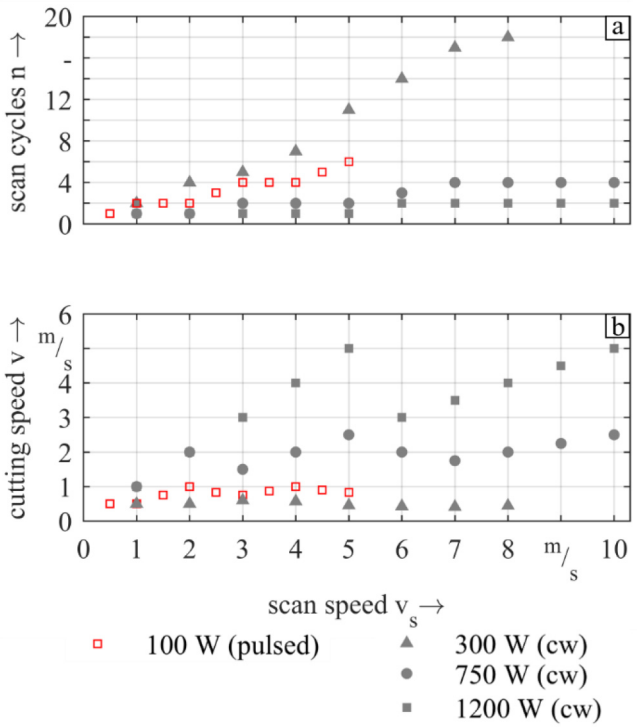

FIG. 4. Scan cycles n for a through cut as a function of the scan speed and the laser power for the cw laser system and the ns pulsed laser system ($f = 500$ kHz) (a) and resulting cutting speeds at different scan speeds (b).

The number of necessary iterations and the cutting speed show a linear relationship from which the total processing speed can be deduced. The results presented in Fig. 4 point out that for the ns pulsed laser system, the overall processing speed could be increased to $v = 0.9$ m/s by implementing a multipass strategy with five scan cycles ($v_S = 4.5$ m/s). Moreover, in comparison to the single-pass strategy, the clearance width could be reduced by 14% to $w_c = 36\,\mu$m (see Table II). In contrast, a substantial reduction of the clearance width by 54% ($w_c = 41\,\mu$m) was achieved for the cw laser system at the expense of productivity, as the respective cutting speed of $v = 2$ m/s is distinctly below the single-pass velocity. However, as the power range of the laser system could not be used completely, the results show that a further increase in the scan speed v_s opens up a great potential for highly focused cw laser sources.

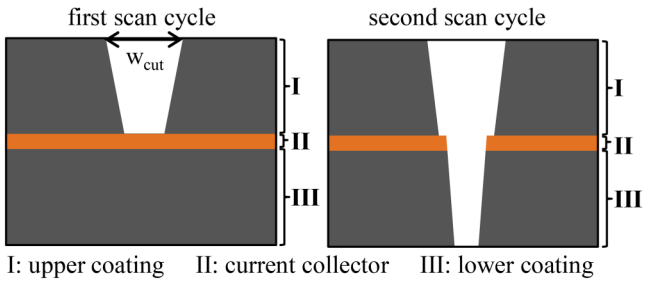

FIG. 5. Illustration of a two-step multipass strategy with variable process parameters; first scan cycle: ablation of the upper coating (I); second scan cycle: ablation of the current collector (II); and the lower coating (III).

In a second approach, the cutting process was divided into two scan cycles with customized processing parameters to further reduce the clearance width. This strategy considers that substantially more energy must be employed for the cutting of the copper layer compared to the graphite coating to account for the differences in the ablation thresholds.[21] The comparably low ablation threshold of the electrode coating results from the ablation mechanism, which is based on the evaporation of the binder and the ejection of entire particles.[38] For this reason, the properties of the first scan cycle were selected to ablate the upper coating with a minimum cutting width w_{cut} as illustrated in Fig. 5.

TABLE II. Cutting speed v and clearance width w_c as obtained with single-pass and multipass strategies for the cw, the ns, and the ps pulsed laser system; for the multipass strategy with variable parameters, two passes (I, II) with different parameter sets were used.

Process strategy	Mode of operation	Laser power P in W	Pulse repetition rate f in kHz	Scanning speed v_S in m/s	Number of scan cycles n	Cutting speed v in m/s	Clearance width w_c in μm
Single-pass	ps	50	1833	0.20	1	0.20	0
	ns	100	500	0.80	1	0.80	42
	cw	2400	–	10.00	1	10.00	90
	cw	300	–	0.25	1	0.25	40
Multipass (constant parameters)	ns	100	500	4.50	5	0.90	36
	ns	100	500	1.50	2	0.75	25
	cw	750	–	8.00	4	2.00	41
	cw	300	–	4.00	7	0.57	38
Multipass (variable parameters)	ns	20	500	0.90	I	0.53	39
	ns	100	500	1.30	II		
	cw	300	–	1.00	I	0.83	34
	cw	750	–	5.00	II		

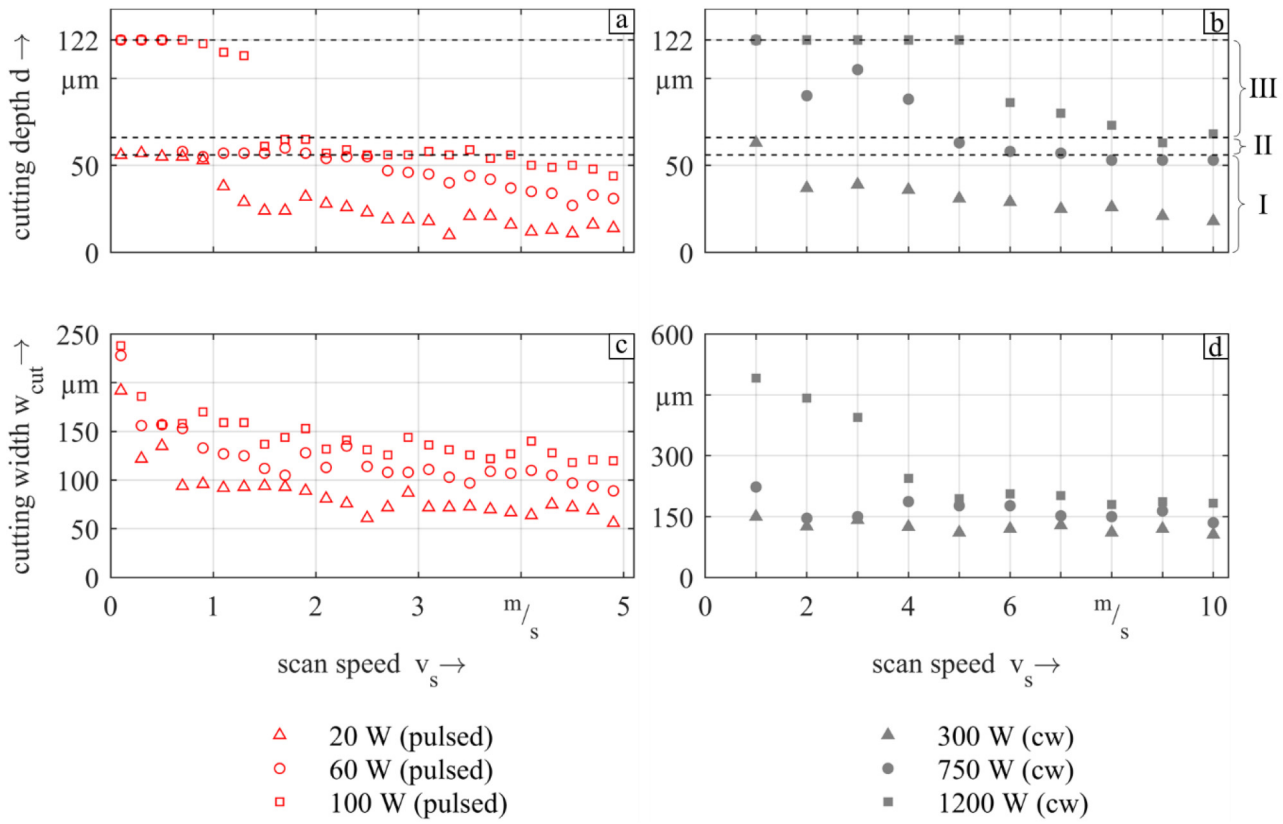

FIG. 6. Determination of the parameter set for the first scan cycle of a multipass strategy with variable parameters; cutting depth [(a) and (b)] and cutting width [(c) and (d)] as a function of the scan speed v_s for the ns pulsed laser system ($f = 500$ kHz, $\tau = 30$ ns) [(a) and (c)] and the cw laser system [(b) and (d)]; I: upper coating, II: current collector, and III: lower coating.

In the first scan cycle, the scan speed was reduced for every power level considered, until the current collector was exposed and a minimal cutting width originated (see Fig. 6). Subsequently, a second scan cycle at increased power and speed was performed, cutting through the current collector and the lower graphite layer. For the ns pulsed laser source, no further improvement in the cutting speed or the clearance width could be realized. The minimum clearance width of 39 μm was attained at a resulting cutting speed of 0.53 m/s (see Table II). Therefore, a scan cycle with a comparatively low laser power of $P = 20$ W ($v_S = 0.9$ m/s) was combined with a scan cycle with a high laser power of 100 W ($v_S = 1.3$ m/s). By contrast, the clearance width achieved with the cw laser system could be reduced to $w_c = 34\,\mu$m by combining a low power and low velocity pass ($P = 300$ W, $v_S = 1$ m/s) with a high power and high velocity pass ($P = 750$ W, $v_S = 5$ m/s). Thus, the resulting cutting speed amounted to $v = 0.83$ m/s.

C. Picosecond laser cutting

The application of ultrashort-pulsed lasers aims at a reduction of the heat input into the electrode material and, thus, at the improvement of the cut edge quality. As illustrated in Fig. 7, laser cutting with a picosecond (ps) laser system improves the cut edge quality significantly. Due to the narrow spot size of 18 μm and the Gaussian intensity profile of the laser beam, small cutting kerfs of around 10 μm were realized with almost no clearance width at all. The modification of the surface around the kerf can be attributed to the removal of entire particles, but the high laser intensities coming from pulse energies of up to 25 μJ also led to the cutting of individual

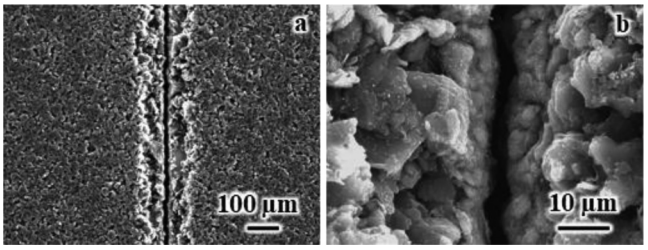

FIG. 7. SEM pictures of a graphite anode with a cutting kerf produced by the ps laser system ($P = 50$ W, $f = 1833$kHz, $v = 0.2$ m/s, $\tau = 2$ ps).

graphite particles. As a consequence, a very low heat input with a superior cutting edge quality can be induced. As this results in considerably less binder evaporation, a higher mechanical stability in the area of the cutting zone can be expected. With the laser system used, the maximum cutting speed for a through cut was $v = 0.2$ m/s.

Since economic ps fiber laser sources with higher power levels and pulse energies are expected in the near future, the potential, especially for applications with particularly high-quality requirements, is apparent.

Selected results obtained from the applied process strategies and the different laser sources are comparatively shown in Table II.

V. CONCLUSION

In this publication, a ns, a ps, and a cw laser systems were compared with regard to their potential application for electrode cutting in LIB production. As in the industrial field, both high throughput and excellent cut edge quality are demanded, the correlation between processing speed and clearance width was investigated. Cutting velocities of up to $v = 10$ m/s were achieved using the cw laser system, which is well above the productivity attainable with pulsed laser sources. Furthermore, the potential of several process strategies was discussed. Significant improvements in the cutting quality were achieved by using multiple scan cycles, especially when applying two scan cycles with individualized parameter sets. The promising results of the cw process indicate the potential of highly focused laser beams in combination with suitable process strategies. Novel scanner technologies, e.g., polygon scanners, reach scan velocities of more than $v_S = 200$ m/s and, therefore, are promising for the industrial implementation of multipass strategies. Additionally, the potential of a ps laser system for high-quality cutting was shown. As the achieved cutting speeds of $v = 0.2$ m/s were still too low for industrial application, ps laser systems with higher repetition rates in combination with a high speed galvanometer or polygon scanners are promising alternatives to established ns laser systems. Furthermore, novel materials in battery production open up a new field for the application of ultrashort-pulsed lasers. For example, for the production of all-solid-state batteries, thermosensitive materials like lithium and solid-state electrolytes need to be processed precisely and with a negligible thermal impact. The results presented in the scope of this work can support production engineers as well as LIB and laser manufacturers in the selection of a suitable laser system as well as in the process design for electrode cutting. Further research is required to assess the impact of the laser cutting parameters on the performance and quality of LIB over their entire lifetime. In particular, the deposition of particles on the electrode surface must be considered for safety reasons.

ACKNOWLEDGMENT

The support of IPG Photonics Corporation for laser processing is gratefully acknowledged by the authors.

REFERENCES

[1]A. Opitz, P. Badami, L. Shen, K. Vignarooban, and A. M. Kannan, "Can Li-ion batteries be the panacea for automotive applications?," Renew. Sustain. Energy Rev. **68**, 685–692 (2017).
[2]G. Zubi, R. Dufo-López, M. Carvalho, and G. Pasaoglu, "The lithium-ion battery: State of the art and future perspectives," Renew. Sustain. Energy Rev. **89**, 292–308 (2018).
[3]G. E. Blomgren, "The development and future of lithium ion batteries," J. Electrochem. Soc. **164**, A5019–A5025 (2017).
[4]S. Michaelis, E. Rahimzei, A. Kampker, H. Heimes, C. Lienemann, C. Offermanns, M. Kehrer, A. Thielmann, T. Hettesheimer, C. Neef, A. Kwade, W. Haselrieder, S. Rahlfs, R. Uerlich, and N. Bognar, *Roadmap Battery Production Equipment 2030: Update 2018* (Frankfurt am Main, Germany, 2018).
[5]A. Kwade, W. Haselrieder, R. Leithoff, A. Modlinger, F. Dietrich, and K. Droeder, "Current status and challenges for automotive battery production technologies," Nat. Energy **3**, 290–300 (2018).
[6]M. Westermeier, G. Reinhart, and M. Steber, "Complexity management for the start-up in lithium-ion cell production," in *ICRM 2014, 2nd International Conference on Ramp-Up Management 2014, CIRP Proceedings, Aachen, Germany, 12–13 June 2014* (Elsevier, Amsterdam, 2014), pp. 13–19.
[7]M. Li, J. Lu, Z. Chen, and K. Amine, "30 years of lithium-ion batteries," Adv. Mater. **30**, 1800561 (2018)
[8]T. Hettesheimer, A. Thielmann, C. Neef, K.-C. Möller, M. Wolter, V. Lorentz, M. Gepp, M. Wenger, T. Prill, J. Zausch, P. Kitzler, J. Montnacher, M. Miller, M. Hagen, P. Fanz, and J. Tübke, *Entwicklungsperspektiven für Zellformate von Lithium-Ionen-Batterien in der Elektromobilität* (Fraunhofer-Allianz Batterien, Pfinztal, 2017).
[9]D. Andre, H. Hain, P. Lamp, F. Maglia, and B. Stiaszny, "Future high-energy density anode materials from an automotive application perspective," J. Mater. Chem. A **5**, 17174–17198 (2017).
[10]D. Andre, S.-J. Kim, P. Lamp, S. F. Lux, F. Maglia, O. Paschos, and B. Stiaszny, "Future generations of cathode materials: An automotive industry perspective," J. Mater. Chem. A **3**, 6709–6732 (2015).
[11]R. Schmuch, R. Wagner, G. Hörpel, T. Placke, and M. Winter, "Performance and cost of materials for lithium-based rechargeable automotive batteries," Nat. Energy **3**, 267–278 (2018).
[12]K. G. Gallagher, S. E. Trask, C. Bauer, T. Woehrle, S. F. Lux, M. Tschech, P. Lamp, B. J. Polzin, S. Ha, B. Long, Q. Wu, W. Lu, D. W. Dees, and A. N. Jansen, "Optimizing areal capacities through understanding the limitations of lithium-ion electrodes," J. Electrochem. Soc. **163**, A138–A149 (2016).
[13]D. Lee, B. Oh, and J. Suk, "The effect of compactness on laser cutting of cathode for lithium-Ion batteries using continuous fiber laser," Appl. Sci. **9**, 205, 1–16 (2019).
[14]T. Jansen, M. W. Kandula, D. Blass, S. Hartwig, W. Haselrieder, and K. Dilger, "Evaluation of the separation process for the production of electrode sheets," Energy Technol. **8**, 1900519, 1–11 (2019).
[15]W. Pfleging, "A review of laser electrode processing for development and manufacturing of lithium-ion batteries," Nanophotonics **7**, 549–573 (2018).
[16]M. Luetke, V. Franke, A. Techel, T. Himmer, U. Klotzbach, A. Wetzig, and E. Beyer, "A comparative study on cutting electrodes for batteries with lasers," Phys. Proc. **12**, 286–291 (2011).
[17]A. H. A. Lutey, A. Fortunato, A. Ascari, S. Carmignato, and C. Leone, "Laser cutting of lithium iron phosphate battery electrodes: Characterization of process efficiency and quality," Opt. Laser Technol. **65**, 164–174 (2015).
[18]T. Günther, D. Schreiner, A. Metkar, C. Meyer, A. Kwade, and G. Reinhart, "Classification of calendering-induced electrode defects and their influence on subsequent processes of lithium-ion battery production," Energy Technol. **8**, 1900026 (2020).
[19]M. Plaimer, C. Breitfuß, W. Sinz, S. F. Heindl, C. Ellersdorfer, H. Steffan, M. Wilkening, V. Hennige, R. Tatschl, A. Geier, C. Schramm, and S. A. Freunberger, "Evaluating the trade-off between mechanical and electrochemical performance of separators for lithium-ion batteries: methodology and application," J. Power Sources **306**, 702–710 (2016).
[20]M. F. Lagadec, R. Zahn, and V. Wood, "Designing polyolefin separators to minimize the impact of local compressive stresses on lithium ion battery performance," J. Electrochem. Soc. **165**, A1829–A1836 (2018).

[21]B. Schmieder, "Laser cutting of graphite anodes for automotive lithium-ion secondary batteries: Investigations in the edge geometry and heat affected zone," Proc. SPIE **8244**, 82440R (2012).
[22]A. Fröhlich, R. Leithoff, C. von Boeselager, K. Dröder, and F. Dietrich, "Investigation of particulate emissions during handling of electrodes in lithium-ion battery assembly," in *CIRPE 2018, 6th CIRP Global Web Conference, 23–25 October 2018* (Elsevier, Amsterdam, 2018), pp. 341–346
[23]J. Kurfer, M. Westermeier, C. Tammer, and G. Reinhart, "Production of large-area lithium-ion cells—Preconditioning, cell stacking and quality assurance," CIRP Ann. Manuf. Technol. **61**, 1–4 (2012).
[24]G. Reinhart, T. Zeilinger, J. Kurfer, M. Westermeier, C. Thiemann, M. Glonegger, M. Wunderer, C. Tammer, M. Schweier, and M. Heinz, "Research and demonstration center for the production of large-area lithium-ion cells," in *Future Trends in Production Engineering*, edited by G. Schuh (Springer, Berlin, 2013), Vol. 12, pp. 3–12.
[25]R. Baumann, A. F. Lasagni, P. Herwig, A. Wetzig, C. Leyens, and E. Beyer, "Efficient separation of battery materials using remote laser cutting-high output performance, contour flexibility, and cutting edge quality," J. Laser Appl. **31**, 022210 (2019).
[26]J. Inderherbergh, "Polyvinylidene fluoride (PVDF) appearance, general properties and processing," Ferroelectrics **115**, 205–302 (1991).
[27]R. Patwa, H. Herfurth, S. Heinemann, J. Mazumder, and D. Lee, "Investigation of different laser cutting strategies for sizing of Li-ion battery electrodes," in *ICALEO 2012, 31st International Congress on Laser Materials Processing, Laser Microprocessing and Nanomanufacturing, Anaheim, CA, 23–27 September 2012* (Laser Institute of America, Orlando, FL, 2012), pp. 908–914
[28]A. G. Demir and B. Previtali, "Remote cutting of Li-ion battery electrodes with infrared and green ns-pulsed fibre lasers," Int. J. Adv. Manuf. Technol. **75**, 1557–1568 (2014).
[29]D. Lee, R. Patwa, H. Herfurth, and J. Mazumder, "Computational and experimental studies of laser cutting of the current collectors for lithium-ion batteries," J. Power Sources **210**, 327–338 (2012).
[30]D. Lee, R. Patwa, H. Herfurth, and J. Mazumder, "Parameter optimization for high speed remote laser cutting of electrodes for lithium-ion batteries," J. Laser Appl. **28**, 022006 (2016).
[31]T. Jansen, M. W. Kandula, S. Hartwig, L. Hoffmann, W. Haselrieder, and K. Dilger, "Influence of laser-generated cutting edges on the electrical performance of large lithium-ion pouch cells," Batteries **5**, 1–20 (2019).
[32]M. R. Kronthaler, F. Schloegl, J. Kurfer, R. Wiedenmann, M. F. Zaeh, and G. Reinhart, "Laser cutting in the production of lithium ion cells," Phys. Procedia **39**, 213–224 (2012).
[33]A. H. A. Lutey, A. Fortunato, S. Carmignato, and M. Fiorini, "High speed pulsed laser cutting of $LiCoO_2$ Li-ion battery electrodes," Opt. Laser Technol. **94**, 90–96 (2017).
[34]T. Reincke, S. Krelinga, and K. Dilgera, "The influences of pulse overlap on cut quality during fiber laser cutting of electrodes for Lithium-ion batteries," in *LIM 2015, Lasers in Manufacturing Conference 2015, Munich, Germany, 22–25 June 2015* (Wissenschaftliche Gesellschaft Lasertechnik, 2015).
[35]X. Liu, D. Du, and G. Mourou, "Laser ablation and micromachining with ultrashort laser pulses," IEEE J. Quantum Electron. **33**, 1706–1716 (1997).
[36]W. Pfleging, M. Mangang, M. Bruns, Y. Zheng, and P. Smyrek, "Laser processes and analytics for high power 3D battery materials," Proc. SPIE **9740**, 974013 (2016).
[37]Y. Zhang, J. Li, R. Yang, T. Liu, and Y. Yan, "Analysis of kerf quality on ultrafast laser cutting of anode material for lithium-ion battery," Opt. Lasers Eng. **118**, 14–21 (2019).
[38]B. Schmieder, "Analytical model of the laser ablation mechanism of lithium-ion battery coatings," Proc. SPIE **9351**, 93511C (2015).

Meet the Authors

Johannes Kriegler is working as a research associate and doctoral candidate at the Institute for Machine Tools and Industrial Management (*iwb*). He studied mechanical engineering at the Technical University of Munich (TUM). His current research focuses on the application of laser technology in the field of battery production and, in particular, on the cutting of thin film battery materials.

Moritz Binzer is a master student in Robotics, Cognition, Intelligence at the Technical University of Munich (TUM). As part of his bachelor thesis, he investigated the laser cutting of lithium-ion battery electrodes using different beam sources. He is currently working as a research assistant at the Institute for Machine Tools and Industrial Management (*iwb*).

Michael F. Zaeh is the head of the Institute for Machine Tools and Industrial Management (*iwb*) as well as a full professor for Machine Tools and Manufacturing Technologies at the Technical University of Munich (TUM). His current fields of research are machine tools, additive manufacturing processes, manufacturing technology, and cognition for technical systems.